Pediatr Cardiol (2008) 29:718–725
DOI 10.1007/s00246-008-9227-y

ORIGINAL ARTICLE

Assessment of Myocardial Function in Pediatric Patients with Operated Tetralogy of Fallot: Preliminary Results with 2D Strain Echocardiography

Walter Knirsch · Ali Dodge-Khatami · Alexander Kadner · Oliver Kretschmar · Johannes Steiner · Petra Böttler · Deniz Kececioglu · Paul Harpes · Emanuela R. Valsangiacomo Buechel

Received: 1 November 2007 / Accepted: 22 March 2008 / Published online: 28 May 2008

Abstract The global myocardial function in patients after repair of tetralogy of Fallot (TOF) can be assessed by cardiovascular magnetic resonance (CMR) and measurement of B-type natriuretic peptides. Two-dimensional echocardiography-derived strain and strain rate (2D strain) facilitate the assessment of regional myocardial function. We evaluated myocardial function in 16 children with residual severe pulmonary valve regurgitation and right ventricular (RV) volume overload after TOF repair before, 1 month after, and 6 months after pulmonary valve replacement (PVR). In 2D strain echocardiography preoperatively, the longitudinal systolic RV strain was reduced ($p < 0.05$). One month after PVR, longitudinal systolic RV strain decreased further ($p < 0.05$), while systolic and early diastolic radial left ventricular strain and strain rate increased (each $p < 0.05$), followed by a return toward preoperative values after 6 months. Six months after PVR, preoperatively elevated RV end-diastolic volume ($p < 0.01$) assessed by CMR and N-terminal pro-B-type natriuretic peptide ($p < 0.05$) decreased. In conclusion, the impairment of the regional myocardial after TOF repair and transient changes after PVR can be subtly analyzed by 2D strain echocardiography in addition to the established assessment of myocardial function with CMR and measurement of B-type natriuretic peptides.

Keywords Echocardiography · Tetralogy of Fallot · Myocardial function

W. Knirsch (✉) · O. Kretschmar · E. R. Valsangiacomo Buechel
Division of Pediatric Cardiology, University Children's Hospital Zurich, Steinwiesstr. 75, 8032 Zurich, Switzerland
e-mail: walter.knirsch@kispi.uzh.ch

A. Dodge-Khatami · A. Kadner
Division of Cardiovascular Surgery, University Children's Hospital Zurich, Zurich, Switzerland

J. Steiner · P. Böttler · D. Kececioglu
Department of Pediatric Cardiology, University Children's Hospital Freiburg, Freiburg, Germany

D. Kececioglu
Clinic for Congenital Heart Defects, Heart and Diabetes Center NRW, Bad Oeynhausen, Germany

P. Harpes
Department of Biostatistics, University of Zurich, Zurich, Switzerland

Introduction

Pulmonary valve dysfunction after surgical repair of patients with tetralogy of Fallot (TOF) is a common problem during long-term follow-up [19]. Pulmonary valve regurgitation causes right ventricular (RV) volume overload leading to RV dysfunction, with an increasing risk for arrhythmias and sudden death [6]. Pulmonary valve replacement (PVR) may become necessary to protect RV function and for remodeling of the RV and left ventricle (LV) [32]. Several methods are available for evaluation of myocardial function, however, advanced assessment of RV function remains a challenge. Cardiovascular magnetic resonance (CMR) has been established to be the gold standard for measuring volume and global systolic function, i.e., the ejection fraction (EF), of both ventricles in adult and pediatric patients after TOF repair [27, 30, 31].

Measurement of B-type natriuretic peptide (BNP) and its N-terminal prohormone (NT-proBNP) has been described as a useful, easy, and fast method for evaluation of global myocardial function in congenital heart disease [13, 28].

Myocardial deformation indexes of strain and strain rate, derived either by tissue Doppler imaging or nowadays, more easily, by 2D strain echocardiography, are an advanced diagnostic modality to quantify regional myocardial function [14, 33]. The aim of our study was to analyze the myocardial function of the RV and LV in pediatric patients with severe pulmonary valve regurgitation after TOF repair before and after PVR by using 2D strain echocardiography in addition to CMR and measurement of BNP.

Methods

Study Population

The study population consisted of 16 pediatric patients (11 male, 5 female) with severe pulmonary valve regurgitation after TOF repair who underwent redo surgery for PVR between May 2004 and May 2006. The mean ± standard deviation age at PVR was 11.7 ± 3.5 years (range: 6.8–19.7 years). Severe pulmonary valve regurgitation was defined at echocardiography as diastolic backflow in the peripheral pulmonary artery side branches by color and pulsed wave Doppler.

All patients had undergone a primary surgical repair of TOF at the age of 1.8 ± 0.9 years (range: 0.3–4.6 years). Two patients had an additional mild to moderate pulmonary valve stenosis (peak systolic Doppler gradient transvalvular, <50 mm Hg). At surgical repair the right ventricular outflow tract was reconstructed with insertion of a homograft in 10 patients and with a transannular patch in 6 patients.

Before PVR, 11 patients were in functional New York Heart Association (NYHA) class I, 5 patients were in NYHA class II, and 2 patients were receiving cardiac medication. All patients were in sinus rhythm and presented a complete right bundle branch block with a QRS duration of 145 ± 25 ms. The indication for PVR was RV dilatation with an indexed RV end-diastolic volume >150 ml/m^2, as measured by CMR [30]. The time interval between surgical repair and redo PVR was 9.9 ± 2.6 years.

The study was approved by the ethical committee of the University of Zurich.

Echocardiography

Transthoracic echocardiography was performed preoperatively, and at 1 and 6 months after PVR using an ultrasound machine (Vivid 7 Pro; GE Vingmed Ultrasound, Norway) with a 3-MHz transducer (3S phased array probe; GE Vingmed Ultrasound). Complete data sets were available for 13 patients. RV and LV end-diastolic diameters were measured in parasternal short axis and apical four-chamber view. The tricuspid valve annulus diameter, right ventricular end-diastolic and end-systolic areas, RV fractional area change, and tricuspid annular motion were measured in the apical four-chamber view. LV end-diastolic and end-systolic volumes and ejection fraction were calculated using a modified Simpson's rule from the apical four-chamber view.

For measurement of the regional myocardial function the myocardial deformation indexes strain and strain rate were calculated. Two-dimensional echocardiographic loops were acquired from the apical four-chamber view for the measurement of the longitudinal function of the RV, the interventricular septum (IVS) and the LV. The apical, mid, and basal segments of the myocardial wall were analyzed. For further statistical analysis a mean value of the three segments was calculated. From the parasternal short-axis view at the level of the papillary muscles, the radial function of the LV was analyzed in the anteroseptal and posterior segments of the LV. The frame rate was between 40 and 80 per second. Three complete cardiac cylces were digitally stored for off-line data analysis. Pulse wave Doppler data were obtained from all four valves for exact timing.

The data were stored in digital format and transferred to a computer workstation (EchoPAC PC SWO; GE Vingmed Ultrasound) for further off-line 2D strain quantitative analysis of the myocardial deformation indexes strain and strain rate.

Due to the lack of 2D strain echocardiography reference values for healthy children, we compared the data for our patients with the data for 10 healthy children (mean age, 14 ± 3.3 years).

Cardiovascular Magnetic Resonance

CMR was performed preoperatively and 6 months postoperatively with a 1.5-T system (Signa MR/I Echo Speed; General Electric Medical Systems, Milwaukee, WI, USA) using a phased-array cardiac coil. Complete data sets were available for 15 patients. One patient was excluded due to loss of follow-up. Images for the assessment of ventricular volumes were acquired using the steady-state free precession sequence with a protocol previously described [30]. The images were acquired during breath holding in all patients. Volumetric data on the ventricles were calculated with the MASS software package (Magnetic Resonance Analytical Software System Version 4.0; MEDIS Medical Imaging Systems, Leiden, The Netherlands). The ejection fractions for the RV and LV were calculated as EF [=(end-diastolic volume – end-systolic volume)/end-diastolic volume × 100]. Normal values in children for ventricular volumes measured by CMR are 67 ± 9 ml/m^2 for the left ventricular end-diastolic volume and 70 ± 11 ml/m^2 for the right ventricular end-diastolic volume using gradient echo

cine CMR [16]. Normal values for the EF measured by CMR are 70 ± 4 % for the RV and 70 ± 6 % for the LV [8].

Measurements of B-Type Natriuretic Peptides

BNP was determined preoperatively and 1 and 6 months after PVR. Three milliliters of heparinized venous blood (N-terminal pro-B-type natriuretic peptide NT pro-BNP) and 2 ml of EDTA venous blood (BNP) were taken from each patient, lying in a supine position for at least 20 min. Blood samples were centrifuged at 3500 *g* for 10 min at 4°C immediately after collection, and plasma separated for NT pro-BNP with electrochemiluminescence immonoassay on a Modular E170 immunoanalyzer (Roche Diagnostics, Mannheim, Germany). BNP measurement was performed with a two-site immunoenzymatic ("sandwich") assay, the Triage BNP assay (Biosite Diagnostic Inc., San Diego, CA, USA). Reference plasma values for NT pro-BNP using this assay were 111 ± 12.5 ng/L for healthy children (age, 4 months–15 years) [18]. For BNP using the Triage assay the mean ± SD were 5.1 ± 3.5 ng/L for healthy boys older than 10 years, and 12.1 ± 9.1 ng/L for healthy girls older than 10 years [10].

Statistics

Values are shown as mean ± SD. Comparisons of variables in the same group were performed using a Wilcoxon signed-rank test. A p value <0.05 was considered statistically significant. Since we have recently published data on interobserver and intraobserver variability in an identical group of patients, we did not repeat such measurements for this study [30].

Results

Clinical Results

There was no postoperative mortality or severe morbidity. For replacement of the pulmonary valve, a bovine vein valved conduit (Contegra; Medtronic Inc., Minneapolis, MN, USA) was used in eight patients, a porcine pulmonic valved conduit (Shelhigh Inc.; Union, NJ, USA) in six patients, and a pulmonic homograft inserted in one patient. The pulmonary valve could be reconstructed in one patient. Concomitant surgical procedures consisted of pericardial patch enlargement of the left pulmonary artery in two patients, intraoperative stenting of the right pulmonary artery in one, and tricuspid annuloplasty in another patient. No other surgical procedures on the RV outflow tract were performed. After PVR, 14 patients presented normal pulmonary valve function, were asymptomatic (NYHA I), and were without any cardiac medications. Two patients developed mild pulmonary valve regurgitation during postoperative follow-up, were in NYHA functional class II, and were treated with an angiotensin-converting enzyme inhibitor (Enalapril). In surface ECG, there was a trend toward a decrease in QRS duration 1 month after PVR (QRS 145 ± 25 vs. QRS 139 ± 19 ms; $p = 0.07$).

Echocardiography

Postoperatively, mild pulmonary valve regurgitation was shown at echocardiography in two patients. Standard echocardiographic parameters are summarized in Table 1. After PVR, there was a significant decrease in

Table 1 Standard echocardiographic parameters in patients before and 1 and 6 months after pulmonary valve replacement in patients after TOF repair

	Preoperative	1 mo postoperative	6 mo postoperative
RVEDD (mm)			
Short–axis view	30.3 ± 6.9[a,b]	19.5 ± 5.1[b]	17.6 ± 5.6[a]
4-chamber view	36.5 ± 6.8[a,b]	28.1 ± 4.3[b]	25.6 ± 2.9[a]
RVFAC (%)	37.1 ± 9.1	35.3 ± 8.5	35.7 ± 13.7
Tricuspid valve annulus diameter (mm)	25.0 ± 3.9[a,b]	19.9 ± 4.8[b]	18.1 ± 3.9[a]
TAM (mm)	16.5 ± 4.3[a]	10.8 ± 2.6	11.5 ± 2.5[a]
LV (mm)			
Short-axis view	35.6 ± 5.6[a]	38.9 ± 4.9	42.2 ± 2.6[a]
4-chamber view	32.9 ± 5.6	33.7 ± 6.0	33.2 ± 6.2
LVEF (%)	56.1 ± 11.2	54.8 ± 3.7	60.7 ± 10.1
Tei index (%)	0.43 ± 0.21	0.47 ± 0.27	0.44 ± 0.20

Note: LV, left ventricle; LVEF, left ventricular ejection fraction; RVFAC, right ventricular fractional area change; RVEDD, right ventricle end diastolic diameter; TAM, tricuspid annular motion

[a] $p < 0.05$, preoperatively vs. 6 months postoperatively

[b] $p < 0.05$, preoperatively vs. 1 month postoperatively

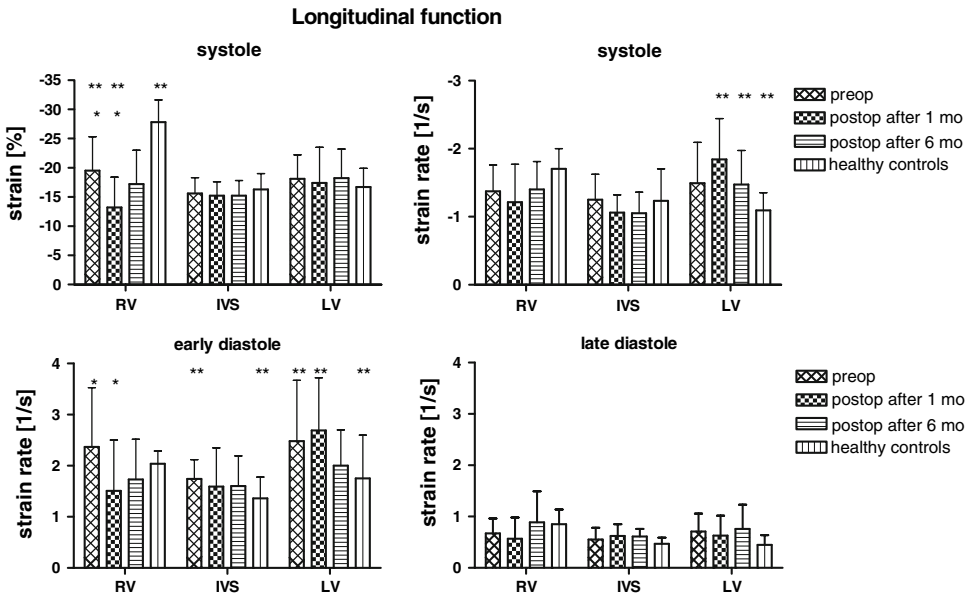

Fig. 1 Two-dimensional echocardiographic-derived (2D strain) myocardial deformation indexes for pediatric patients before and 1 and 6 months after pulmonary valve replacement in patients after tetralogy of Fallot repair and healthy controls. Values for strain and strain rate for the longitudinal function of the right ventricle (RV), interventricular septum (IVS), and left ventricle (LV). *$p < 0.05$, preoperatively (preop) vs. 1 month (mo) postoperatively (postop). **$p < 0.05$, healthy controls vs. patients before and 1 and 6 months postoperatively

RV size, either measured as the RV end-diastolic diameter in short-axis view ($p < 0.05$) or measured in the four-chamber view ($p < 0.01$). Parallel to the decrease in RV size, the tricuspid valve annulus diameter decreased significantly ($p < 0.05$) during postoperative follow-up, while the RV fractional area change did not change. The tricuspid annulus movement (TAM) decreased after PVR ($p < 0.05$). The systolic, early diastolic, and late diastolic strain and strain rate for the longitudinal function of the RV, the IVS, and the LV are shown in Fig. 1, and those for the radial function of the LV in Fig. 2.

Two-Dimensional Strain of the Right Ventricle

The longitudinal systolic strain values of the RV were lower compared to those of healthy controls ($-19.5 \pm 5.8\%$ vs. $-27.8 \pm 3.8\%$; $p < 0.05$) (Fig. 1). One month after PVR, there was a further decrease in the longitudinal systolic RV strain ($-19.5 \pm 5.8\%$ vs. $-13.2 \pm 5.2\%$; $p < 0.05$) and the longitudinal early diastolic RV strain rate (2.37 ± 1.16 vs. 1.51 ± 0.99 s^{-1}; $p < 0.05$). Six months after PVR, the longitudinal RV strain and strain rate in systole, early diastole and late diastole increased but did not reach the preoperative level (Fig. 1).

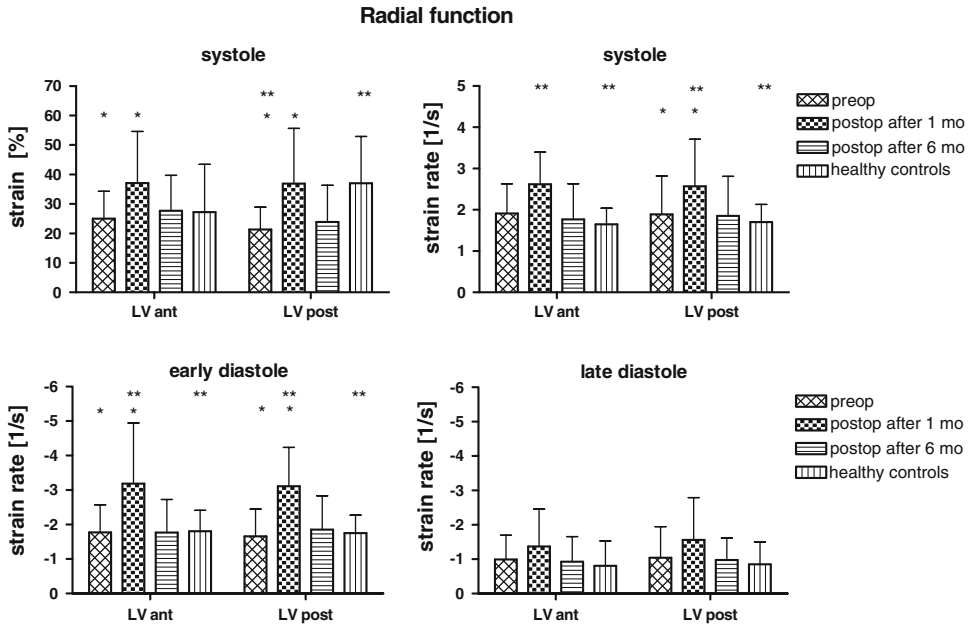

Fig. 2 Two-dimensional echocardiographic-derived (2D strain) myocardial deformation indexes for pediatric patients before and 1 and 6 months after pulmonary valve replacement in patients after tetralogy of Fallot repair and healthy controls. Values for strain and strain rate for the radial function of the left ventricle were analyzed for the anteroseptal (LV ant) and posterior (LV post) segments. *$p < 0.05$, preoperatively (preop) vs. 1 month (mo) postoperatively (postop); **$p < 0.05$, healthy controls vs. patients before and 1 and 6 months postoperatively

Two-Dimensional Strain of the Left Ventricle

The preoperative longitudinal and radial systolic, early diastolic, and late diastolic strain and strain rate of the LV were at least comparable to the values of the healthy controls; the longitudinal early diastolic strain rate was even higher compared to the healthy controls (2.48 ± 1.19 vs. 1.75 ± 0.85 s^{-1}; $p < 0.05$) (Fig. 1). Only the systolic radial LV posterior strain was preoperatively reduced in comparison to those of healthy controls ($21.3 \pm 7.6\%$ vs. $37.0 \pm 15.9\%$; $p < 0.05$) (Fig. 2). One month after PVR there was an increase in the radial systolic LV anteroseptal strain ($25.0 \pm 9.3\%$ vs. $37.1 \pm 17.5\%$; $p < 0.05$), LV posterior strain ($21.3 \pm 7.6\%$ vs. $36.9 \pm 18.7\%$; $p < 0.05$) as well as of the LV posterior strain rate (1.89 ± 0.93 vs. 2.57 ± 1.14 s^{-1}; $p < 0.05$). During diastole the early diastolic radial strain rate both anteroseptal (-1.77 ± 0.80 vs. -3.18 ± 1.76 s^{-1}; $p < 0.05$) and radial posterior (-1.65 ± 0.79 vs. -3.11 ± 1.12 s^{-1}; $p < 0.05$) increased. Compared to healthy controls 1 month after PVR there was an elevated radial systolic LV posterior strain rate (2.57 ± 1.14 vs. 1.70 ± 0.43 s^{-1}; $p < 0.05$), an elevated radial early diastolic LV anterior strain rate (-3.18 ± 1.76 vs. -1.80 ± 0.61 s^{-1}; $p < 0.05$), and LV posterior strain rate (-3.11 ± 1.14 vs. -1.75 ± 0.52; $p < 0.05$). Six months after PVR, the strain and strain rate of the LV returned to preoperative levels (Fig. 2).

Two-Dimensional Strain of the Intraventricular Septum

The longitudinal systolic, early diastolic, and late diastolic strain and strain rate of the IVS in the patient group were comparable to those in healthy controls (Fig. 1).

Cardiovascular Magnetic Resonance Imaging

Table 2 reports the results of CMR before and 6 months after PVR. Before PVR, all patients with severe pulmonary valve regurgitation at echocardiography correspondingly presented a regurgitation fraction larger than 30% at CMR. After PVR, CMR did not demonstrate any significant regurgitant flow just above the pulmonary valve. There was a significant decrease in RV end-diastolic volume, while LV end-diastolic volume remained stable during follow-up. The ejection fraction as a parameter for the global systolic function of the RV and LV did not change significantly.

Measurements of B-Type Brain Natriuretic Peptides

The changes in BNP and NT-proBNP before and 1 and 6 months after PVR are illustrated in Table 2. During postoperative follow-up, NT-proBNP decreased continuously and was significantly lower 6 months after PVR compared to preoperative values.

Discussion

Our study provides preliminary results of the use of 2D strain echocardiography for assessment of myocardial function in pediatric patients with severe pulmonary valve regurgitation after TOF repair, in addition to the established techniques of CMR and measurement of BNPs. Beside a relief of the global myocardial function, as demonstrated by the reduction in RV volume in CMR and decrease in BNPs, we found regional abnormalities of myocardial function, particularly in the longitudinal direction in the RV in 2D strain echocardiography. In contrast, longitudinal and radial function of the LV were preserved.

Ultrasonic strain and strain rate imaging was established as a scientific tool for quantifying regional myocardial function in the late 90s [26, 29] and has been extensively validated in different clinical settings including assessment of regional RV function [9]. While the first commercially available tool was based on tissue Doppler-derived strain

Table 2 Results for cardiovascular magnetic resonance and B-type natriuretic peptides in patients before and 1 and 6 months after pulmonary valve replacement in patients after TOF repair

	Preoperative	1 mo postoperative	6 mo postoperative
CMR RVEDV (ml/m^2)	201 ± 47[a]	–	109 ± 15[a]
LVEDV (ml/m^2)	82 ± 17	–	82 ± 17
RV EF (%)	45 ± 6	–	42 ± 8
LV EF (%)	52 ± 8	–	54 ± 9
Natriuretic peptides NT-ProBNP (ng/L)	182 ± 131[a]	141 ± 78	108 ± 81[a]
BNP (ng/L)	40 ± 24	39 ± 25	36 ± 25

Note: BNP, B-type natriuretic peptide; CMR, cardiovascular magnetic resonance; LVEDV, left ventricular enddiastolic volume; LVEF, left ventricular ejection fraction; NT-proBNP, N-terminal pro-B-type natriuretic peptide; RVEDV, right ventricular enddiastolic volume; RVEF, right ventricular ejection fraction

[a] $p < 0.05$ preoperatively vs. 6 months postoperatively

and strain rate measurements, we used the second generation of 2D echocardiography-derived strain and strain rate technique (2D strain). This technique is based on a gray-scale analysis of one 2D echocardiographic loop throughout the complete cardiac cycle by pixel tracking and has been validated in vitro and in vivo [12]. The advantages of the new 2D strain technique are the simultaneous analysis of radial and longitudinal myocardial deformation in two dimensions, the independence of the insonation angle, and the time-saving practical usability, overcoming the need for manual tracking of each myocardial wall segment throughout the cardiac circle.

Preoperative Assessment of Myocardial Function

CMR and other more invasive techniques such as radionuclide angiocardiography [7, 24] may be helpful for assessing global myocardial function during long-term follow-up after TOF repair both in adults [20, 27, 31] and in adolescents [17, 30] and differentiating the effects of volume versus pressure overload of the RV [2, 20, 28]. However, in contrast, 2D strain echocardiography provides a careful analysis of regional myocardial function. Our data show impaired regional RV myocardial function, with a reduced longitudinal systolic strain of the RV free wall compared to that in healthy controls. In addition, we found an isolated impairment of the radial systolic LV posterior strain. This impairment of the regional myocardial function for both the RV and the LV in pediatric patients after TOF repair was recently shown by Weidemann et al. using Doppler myocardial velocity-derived strain and strain rate [33]. Weidemann et al. found RV deformation abnormalities associated with electrical depolarization abnormalities [33]. Thus, similarly, the isolated preoperative impairment of the radial systolic LV posterior strain that we observed may be correlated with the presence of complete right bundle branch block and, therefore, with interventricular dyssynchrony.

Preoperatively, we measured an elevation of both analyzed types of natriuretic peptides compared to reference values [10, 18]. Previous studies demonstrated that the stimulus for secretion of natriuretic peptides is myocyte stretch due to RV volume overload in severe pulmonary valve regurgitation [13, 15]. Elevated BNP compared to NT-pro-BNP values were found in asymptomatic adult patients as well as pediatric patients after TOF repair [1, 18].

Postoperative Findings

The hemodynamic effect of RV volume unloading after PVR has been demonstrated, with a significant reduction in RV volume in CMR and a significant decrease in BNP levels as previously reported for adults and adolescents [27, 30]. Despite this reduction in the preoperative elevated RV end-diastolic volume, the RV global function ejection fraction, expressed as EF, did not change significantly; this may represent an overestimation of the measured EF preoperatively due to severe pulmonary regurgitation, and some authors have suggested the introduction of a corrected EF [20]. Nevertheless, a similar finding was recently described by Coats et al., who analyzed the hemodynamic effects of percutaneous PVR and postulated that the RV is on the decompensatory limb of the Starling curve before percutaneous PVR and recovers by a leftward shift back to the compensatory limb of the Starling curve after percutaneous PVR [3].

One and six months after PVR, the continuous decrease in the preoperatively elevated BNPs was more pronounced for NT-proBNP than for BNP (Table 2). Due to the longer half-life period and the higher plasma levels of NT-proBNP compared with BNP, management of patients with chronic heart failure and monitoring of the response to therapy with NT-proBNP seem to be more appropriate. In contrast, BNP is more suitable for evaluation of acute hemodynamic changes [22].

Assessment of myocardial function by 2D strain echocardiography demonstrates that the remodeling process of myocardial function is different for the LV and the RV and dependent on the time interval after surgery. The transient deterioration of longitudinal RV function postoperatively may be related to the positive correlation between the regional systolic strain and the stroke volume [26, 34]. The volume overload of the RV is acutely resolved at the time of PVR, leading to an acute decrease in RV stroke volume and, therefore, to a decreased longitudinal RV strain. The following improvement observed 6 months after PVR represents recovery of the RV function from the perioperative trauma [35]. Unlike for the RV, we observed an impairment of radial LV function 1 month after PVR; this may be explained by improved interventricular interaction after reduction of the RV volume, leading to a higher LV filling capacity [4].

The myocardial function of the IVS was similar to that of healthy controls and remained unchanged during the postoperative course; this observation is comparable to the results of other studies, with preservation of the IVS myocardial function in the presence of reduced myocardial function [25].

Potential reasons for the impairment of regional myocardial function observed in our and other studies in patients after TOF repair are multiple and might be related to the surgical trauma, the effect of cardiopulmonary bypass, inborn abnormal ventricular myoarchitecture, chronic hypoxia, and residual postoperative defects [23]. All these factors may contribute to the development of

myocardial fibrosis [11, 12, 35], however, their influence on the different strain directions still needs to be accurately investigated to be completely understood.

Limitations

This study presents only preliminary data based on a small number of subjects. CMR techniques developed to evaluate regional wall motion, including myocardial tagging and tissue phase mapping, have been described; however, their use has so far been limited to adult patients in a research setting [21, 36] These sequences are technically challenging, and postprocessing of the data cumbersone; for these reasons they have not yet been implemented in our pediatric cardiovascular MRI program. Therefore, we were not able to compare the data obtained by echo with those from another technique such as CMR, as reported by other groups [5].

Similarly, no information was available about areas of delayed enhancement potentially detectable by MRI. For all these reasons our preliminary data certainly need confirmation, and new prospectively planned studies assessing a larger number of patients and comparing the results of different methods need to be performed. As long as more robust data are not obtained and better understood, each piece of information should be used to complement the rest, and a clinical decision not made on the basis of one single exam.

Conclusion

Our preliminary data suggest that 2D strain echocardiography offers new opportunities to analyze regional myocardial function in patients after TOF repair. Implementing established methods for assessment of global myocardial function, such as CMR and BNP levels, with such advanced echocardiographic techniques for evaluating regional myocardial function may provide better a understanding of hemodynamics in volume-overloaded ventricles.

Acknowledgments This study was supported by a grant from the University of Zurich, Switzerland. We thank the parents and their children for their participation.

References

1. Brili S, Alexopoulos N, Latsios G, Aggeli C, Barbetseas J, Pitsavos C, Vyssoulis G, Stefanidis C (2005) Tissue doppler imaging and brain natriuretic peptide levels in adults with repaired tetralogy of Fallot. J Am Soc Echocardiogr 18:1149–1154
2. Coats L, Khambadkone S, Derrick G, Sridharan S, Schievano S, Mist B, Jones R, Deanfield JE, Pellerin D, Bonhoeffer P, Taylor AM (2006) Physiological and clinical consequences of relief of right ventricular outflow tract obstruction late after repair of congenital heart defects. Circulation 113:2037–2044
3. Coats L, Khambadkone S, Derrick G, Hughes M, Jones R, Mist B, Pellerin D, Marek J, Deanfield JE, Bonhoeffer P, Taylor AM (2007) Physiological consequences of percutaneous pulmonary valve implantation: the different behaviour of volume- and pressure-overloaded ventricles. Eur Heart J 28:1886–1893
4. Davlouros PA, Kilner PJ, Hornung TS, Li W, Francis JM, Moon JC, Smith GC, Tat T, Pennell DJ, Gatzoulis MA (2002) Right ventricular function in adults with repaired tetralogy of Fallot assessed with cardiovascular magnetic resonance imaging: detrimental role of right ventricular outflow aneurysms or akinesia and adverse right-to-left ventricular interaction. J Am Coll Cardiol 40:2044–2052
5. Delfino JG, Bhasin M, Cole R, Eisner RL, Merlino J, Leon AR, Oshinski JN (2006) Comparison of myocardial velocities obtained with magnetic resonance phase velocity mapping and tissue Doppler imaging in normal subjects and patients with left ventricular dyssynchrony. J Magn Reson Imaging 24:304–311
6. Gatzoulis MA, Balaji S, Webber SA, Siu SC, Hokanson JS, Poile C, Rosenthal M, Nakzawa M, Moller JH, Gillette PC, Webb GD, Redington AN (2000) Risk Factors for arrhythmia and sudden cardiac death late after repair of tetralogy of Fallot: a multicentre study. Lancet 356:975–981
7. Hausdorf G, Hinrichs C, Nienaber CA, Schark C, Keck EW (1990) Left ventricular contractile state after surgical correction of tetralogy of Fallot: risk factors for late left ventricular dysfunction. Pediatr Cardiol 11:61–68
8. Helbing WA, Rebergen SA, Malliepaard C, Hansen B, Ottenkamp J, Reiber JHC, de Roos A (1995) Quantification of right ventricular function with magnetic resonance imaging in children with normal hearts and with congenital heart disease. Am Heart J 130:828–837
9. Jamal F, Bergerot C, Argaud L, Loufouat J, Ovize M (2003) Longitudinal strain quantitates regional right ventricular contractile function. Am J Physiol Heart Circ Physiol 285:H2842–H2847
10. Koch A, Singer H (2003) Normal values of B type natriuretic peptide in in infants, children, and adolescents. Heart 89:875–878
11. Lange PE (1989) Long-term results following surgical treatment of tetralogy of Fallot. Z Kardiol 78 (Suppl 7):47–51
12. Langeland S, D'hooge J, Wouters PF, Leather A, Claus P, Bijnens B, Sutherland GR (2005) Experimental validation of a new ultrasound method for the simultaneous assessment of radial and longitudinal myocardial deformation independent of insonation angle. Circulation 112:2157–2162
13. Law YM, Keller BB, Feingold BM, Boyle GJ (2005) Usefulness of plasma B-type natriuretic peptide to identify ventricular dysfunction in pediatric and adult patients with congenital heart disease. Am J Cardiol 95:474–478
14. Leitman M, Lysayansky P, Sidenko S, Shir V, Peleq E, Binenbaum M, Kaluski E, Krakover R, Vered Z (2004) Two-dimensional strain—a novel software for real-time quantitative echocardiographic assessment of myocardial function. J Am Soc Echocardiogr 17:1021–1029
15. Levin ER, Gardner DG, Samson WK (1998) Natriuretic peptides. N Engl J Med 339:321–328
16. Lorenz CH (2000) The range of normal values of cardiovascular structures in infants, children, and adolescents measured by magnetic resonance imaging. Pediatr Cardiol 21:37–46
17. Niezen RA, Helbing WA, van der Wall EE, van der Geest RJ, Rebergen SA, Roos A (1996) Biventricular systolic function and mass studied with MR imaging in children with pulmonary regurgitation after repair for tetralogy of Fallot. Radiology 201:135–140
18. Nir A, Bar-Oz B, Perles Z, Brooks R, Korach A, Rein AJJT (2004) N-terminal pro-B-type natriuretic peptide: reference

plasma levels from birth to adolescence: elevated levels at birth and in heart diseases. Acta Paediatr 93:603–607
19. Oechslin EN, Harrison DA, Harris L, Downar E, Webb GD, Siu SS, Williams WG (1999) Reoperation in adults with repair of Tetralogy of Fallot: indications and outcomes. J Thorac Cardiovasc Surg 118:245–251
20. Oosterhof T, Tulevski II, Vliegen HW, Spijkerboer AM, Mulder BJ (2006) Effects of volume and/or pressure overload secondary to congenital heart disease (tetralogy of Fallot or pulmonary stenosis) on right ventricular function using cardiac magnetic resonance and B-type natriuretic peptide levels. Am J Cardiol 97:1051–1055
21. Petersen SE, Jung BA, Wiesmann F, Selvanayagam JB, Francis JM, Hennig J, Neubauer S, Robson MD (2006) Myocardial tissue phase mapping with cine phase-contrast MR imaging: regional wall motion analysis in healthy volunteers. Radiology 238:816–826
22. Rodeheffer RJ (2004) Measuring plasma B-type natriuretic peptide in heart failure: good to go in 2004? J Am Coll Cardiol 44:740–749
23. Sanchez-Quintana D, Anderson RH, Ho SY (1996) Ventricular myoarchitecture in tetralogy of Fallot. Heart 76:280–286
24. Schamberger MS, Hurwitz RA (2000) Course of right and left ventricular function in patients with pulmonary insufficiency after repair of Tetralogy of Fallot. Pediatr Cardiol 21:244–248
25. Solarz DE, Witt SA, Glascock BJ, Jones FD, Khoury PR, Kimball TR (2004) Right ventricular strain and strain rate analysis in patients with repaired tetralogy of Fallot: possible interventricular septum compensation. J Am Soc Echocardiogr 17:338–344
26. Sutherland GR, Di Salvo G, Claus P, D'hooge J, Bijnens B (2004) Strain and strain rate imaging: a new clinical approach to quantifying regional myocardial function. J Am Soc Echocardiogr 17:788–802
27. Therrien J, Provost Y, Merchant N, Williams W, Colman J, Webb G (2005) Optimal timing for pulmonary valve replacement in adults after tetralogy of fallot repair. Am J Cardiol 95:779–782
28. Tulevski II, Hirsch A, Dodge-Khatami A, Stoker J, van der Wall EE, Mulder BJ (2003) Effect of pulmonary valve regurgitation on right ventricular function in patients with chronic right ventricular pressure overload. Am J Cardiol 92:113–116
29. Urheim S, Evardsen T, Torp H, Angelsen B, Smiseth OA (2000) Myocardial strain by doppler echocardiography—validation of a new method to quantify regional myocardial function. Circulation 102:1158–1164
30. Valsangiacomo Buechel ER, Dave HH, Kellenberger CJ, Dodge-Khatami A, Pretre R, Berger F, Bauersfeld U (2005) Remodelling of the right ventricle after early pulmonary valve replacement in children with repaired tetralogy of Fallot: assessment by cardiovascular magnetic resonance. Eur Heart J 26:2721–2727
31. Vliegen HW, van Straten A, de Roos A, Roest AA, Schoof PH, Zwindermann AH, Ottenkamp J, van der Wall EE, Hazekamp MG (2002) Magnetic resonance imaging to assess the hemondynamic effects of pulmonary valve replacement in adults repair of tetralogy of fallot. Circulation 106:1703–1707
32. Warner KG, O'Brian PKH, Rhodes J, Kaur A, Robinson DA, Payne DD (2003) Expanding the indications for pulmonary valve replacement after repair of Tetralogy of Fallot. Ann Thorac Surg 76:1066–1072
33. Weidemann F, Eyskens B, Mertens L, Dommke C, Kowalski M, Simmons L, Claus P, Binjes B, Gewellig M, Hatle L, Sutherland GR (2002) Quantification of regional right and left ventricular function by ultrasonic strain rate and strain indexes after surgical repair of tetralogy of Fallot. Am J Cardiol 90:133–138
34. Weidemann F, Jamal F, Sutherland GR, Claus P, Kowalski M, Hatle L, De Scheerder I, Bijnens B, Rademakers FE (2002) Myocardial function defined by strain rate and strain during alterations in inotropic states and heart rate. Am J Physiol Heart Circ Physiol 283:H792–H799
35. Wranne B, Pinto FJ, Hammarstrom E, St Goar FG, Puryear J, Popp RL (1991) Abnormal right heart filling after cardiac surgery: time course and mechanisms. Br Heart J 66:435–442
36. Young AA, Imai H, Chang CN, Axel L (1994) Two-dimensional left ventricular deformation during systole using magnetic resonance imaging with spatial modulation of magnetization. Circulation 89:740–752